# National Institute of Standards & Technology

# Certificate of Analysis

## Standard Reference Material® 2012

### Calibration Standard for High-Resolution X-Ray Diffraction

(200 mm Wafer)

This Standard Reference Material (SRM) provides the high-resolution X-ray diffraction (HRXRD) community with Si (220) *d*-spacing in transmission, surface-to-crystal-plane wafer miscut, and surface-to-Si (004) Bragg angle in reflection traceable to the International System of Units (SI) [1] for our reference wavelength. A unit of SRM 2012 consists of a 200 mm diameter × 0.725 mm thick double-polished (100)-oriented, single-crystal Si wafer with a nominal 50 nm $Si_{0.85}Ge_{0.15}$ epitaxial layer and 25 nm Si cap. These certified values can be used to calibrate HRXRD instrumentation.

Table 1. Certified Values for SRM 2012

| Quantity[(a)] | Certified Value | | Expanded Uncertainty[(b)], $U$ for $k = 2$ | |
|---|---|---|---|---|
| $d_{SRM}$ | 0.192 016 1 | nm (at 22.5 °C) | 0.000 000 9 | nm |
| $\xi_{SRM}$ | 4.360 | mrad | 0.027 | mrad |
| $\phi_{SRM}$ | –360 | mrad | 16 | mrad |
| $x_{SRM}$ | –1.534 | mrad | 0.072 | mrad |
| $y_{SRM}$ | 4.081 | mrad | 0.019 | mrad |
| $\theta_{surface,SRM(004)}$ | 0.604 785 | rad | 0.000 076 | rad |

[(a)] The identity of the quantity is defined in Table 2.
[(b)] For methods used to calculate uncertainties, see references 2 through 4.

**Expiration of Certification:** The certification of **SRM 2012** is valid indefinitely, within the measurement uncertainty specified, provided the SRM is handled and stored in accordance with the instructions given in this certificate (see "Instructions for Handling, Storage, and Use"). Accordingly, periodic recalibration or recertification of this SRM is not required. The certification is nullified if the SRM is damaged, contaminated, or otherwise modified.

**Maintenance of SRM Certification:** NIST will monitor this SRM over the period of its certification. If substantive technical changes occur that affect the certification before the expiration of this certificate, NIST will notify the purchaser. Registration (see attached sheet) will facilitate this notification.

The overall coordination of the preparation and technical direction of the certification were performed by J.P. Cline of the NIST Ceramics Division. Realization of the instrumental capability, development of the experimental design, and collection of measurement data were performed by D. Windover of the NIST Ceramics Division. D.L. Gil, a guest researcher for the NIST Ceramics Division, analyzed the data to certified parameters. Hardware design and alignment procedures were facilitated by A. Henins of the NIST Ceramics Division.

Statistical analysis was provided by J. Filliben of the NIST Statistical Engineering Division.

Support aspects involved in the issuance of this SRM were coordinated through the NIST Measurement Services Division.

Debra L. Kaiser, Chief
Ceramics Division

Gaithersburg, MD 20899
Certificate Issue Date: 27 January 2012

Robert L. Watters, Jr., Chief
Measurement Services Division

**Supporting contributions to SRM certification:** K. Bowen of Bede X-Ray Metrology, Denver, CO, provided key advice in the development of the HRXRD test structure. M. Wormington of Bede X-Ray Metrology and L. Bruegemann of Bruker AXS, Karlsruhe, Germany, provided supporting HRXRD measurements on the SRM feedstock. D. Black of the Ceramics Division at NIST performed X-ray topographs at the XOR/UNICAT facility at the Advanced Photon Source, Argonne, IL. R. Gates of the Ceramics Division at NIST performed SEM images at the NanoFab Facility at the NIST Center for Nanoscale Science and Technology (CNIST). Applied Materials, Santa Clara, CA, deposited $Si_{1-x}Ge_x$ epitaxial structures as a custom service for NIST.

Table 2. Definitions of the Certified Values for SRM 2012

| Quantity | Description |
|---|---|
| $d_{SRM}$ | Si (220) transmission case *d*-spacing |
| $\xi_{SRM}$ | Magnitude of wafer miscut (polar form) |
| $\phi_{SRM}$ | Direction of wafer miscut (polar form) |
| $x_{SRM}$ | Tilt of wafer miscut in *x*-plane (Cartesian form) |
| $y_{SRM}$ | Tilt of wafer miscut in *y*-plane (Cartesian form) |
| $\theta_{surface,SRM(004)}$ | Angle from wafer surface of Si (004) reflection peak |

**Material Description[(1)]:** The SRMs were selected from a series of 25 type-p, B-doped, 200 mm Czochralski (CZ) Si wafers manufactured by ShinEtsu, SEH America, Vancouver, WA. A nominal 25 nm Si surface layer was deposited on each wafer, capping a strained, epitaxial, nominal 50 nm $Si_{0.85}Ge_{0.15}$ thin film on one of the polished substrate surfaces (referred to as the "front" surface) using a Centura RP Epi deposition system by the applications lab at Applied Materials. HRXRD measurements were performed on 24 areas (4 rows × 6 columns) within a 150 mm × 100 mm rectangle on each wafer. Each wafer has four quadrant scribe lines at the edges indicating the (110) crystal orientation directions. These scribe lines provide a more accurate orientation reference than the wafer notch. The wafer notch is taken as $\phi = 0$ rad for miscut orientation referencing. (Note that the central 150 mm × 100 mm is the region for which the certified values listed in Table 1 are applicable.)

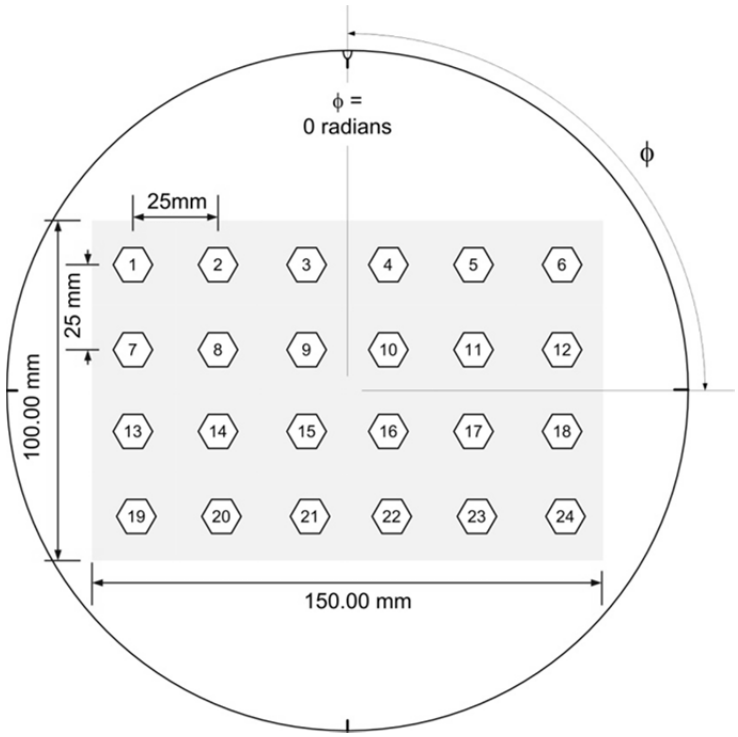


Figure 1. Schematic of wafer showing measurement locations and azimuth, $\phi$, convention for miscut orientation.

[(1)] Certain commercial equipment, instruments, or materials are identified in this certificate to adequately specify the experimental procedure. Such identification does not imply recommendation or endorsement by the National Institute of Standards and Technology, nor does it imply that the materials or equipment identified are necessarily the best available for the purpose.

**MEASUREMENT PROCEDURE**

*D-spacing and Bragg angle measurements:* The NIST approach for establishing SI traceability in HRXRD measurements uses a Si reference crystal of known *d*-spacing and compares it to the wafer feedstock values by a difference method to eliminate significant uncertainties arising from a number of systematic errors. The reference crystal used in this study was cut from a piece of the WASO 04 boule of silicon grown for the Avogadro Project, and polished to a strain-free 450 μm thickness lamella as discussed in reference 5. The (220) lattice spacing has been determined with a combined relative standard uncertainty of $u_c(\Delta d_{WASO04})/d_{WASO04} \leq 6\times10^{-8}$ by the $\Delta d$ lattice comparator at NIST [6–9]. This reference crystal was measured after system alignment changes so that wafer feedstock and reference crystal measurements could be paired only for identical system configurations. The following iterative measurement and analysis approach was followed:

1. Align HRXRD instrument (see alignment methods [10–14]),
2. Measure Si reference crystal with HRXRD instrument,
3. Measure Si wafer feedstock with HRXRD instrument at all sample positions, and
4. Use reference data to provide SI traceability for wafer measurements.

Interpretation of a single diffraction measurement on an HRXRD instrument requires substantial knowledge about instrument alignment and goniometer orientation. One way to eliminate some of the uncertainty resulting from measuring instrument-related parameters is to measure two diffraction features from the same family of planes, ideally the non-dispersive and dispersive settings of the same planes and approximately the same *d*-spacing of the planes used in the instrument's monochromator. (For a treatment of dynamical diffraction theory, see references 15 and 16.) Our approach uses the (220) family to provide information on the Si substrate *d*-spacing. The Bragg angle, $\theta_{B(220)}$, can be accurately determined by measuring the angles of the diffraction peak in each of the crystal's two settings. The angle between the diffracting conditions for the sample will be equal to $2\theta_{B(220)}$, since a diffraction peak is observed at both plus, (220)+, and minus, (220)–, the Bragg angle from a [100]-faceted Si crystal.

$$\theta_{B(220)} = \frac{\left|\theta_{meas(220)+} - \theta_{meas(220)-}\right|}{2} \tag{1}$$

This approach to measuring *d*-spacing is commonly known as the Bond method [17–21]. This method is typically used in a reflection geometry, in which corrections for index of refraction and many other effects are necessary [22]. In contrast, the reference crystal and SRM wafer measurements have been taken in a transmission geometry to eliminate uncertainties related to these corrections. The impact of wafer radius-of-curvature and strain effects on *d*-spacing determination is largely unexplored [23–25], but such effects should affect both certification measurements and subsequent measurements similarly.

Each 200 mm wafer was measured at the 24 central points of the SRM specimens. At each point, or sample position, a step-scan was taken for both the non-dispersive and dispersive Si (220) transmission peaks and for the Si (004) reflection peak from the Si substrate bulk. A longer angular range scan of the Si (004) and $Si_{1-x}Ge_x$ (004) reflection peaks was made to measure properties of the epitaxial surface structure. Table 3 provides the details of these scans. This sequence of scans was performed at least twice at each of the 24 points.

Table 3. Scan Angular Ranges for SRM Measurements

| Scan Type | Range (rad) | Steps | Count Time (s) |
|---|---|---|---|
| Non-dispersive Si (220) | $4.3\times10^{-4}$ | 200 | 2.0 |
| Non- dispersive Si (220) setup | $4.3\times10^{-3}$ | 50 | 1.0 |
| Dispersive Si (220) | $4.3\times10^{-4}$ | 100 | 2.0 |
| Dispersive Si (220) setup | $4.3\times10^{-3}$ | 50 | 1.0 |
| Reflection Si (004) | $4.3\times10^{-4}$ | 100 | 1.0 |
| Reflection Si (004) setup | $4.3\times10^{-3}$ | 50 | 1.0 |
| Reflection Si (004) long | $2.6\times10^{-2}$ | 500 | 5.0 |

*Miscut Measurements:* The measurements used for the certification of $d_{SRM}$ were collected with the wafer notch facing up, $\phi = 0$ rad. The wafers were then rotated to $\phi = \pi/2$ rad, $\pi$ rad, and $3\pi/2$ rad orientations. At least two reflection (004) scans were collected at each azimuthal orientation to determine $\theta_\phi$. Equations 2 and 3 show the calculations used for determining two miscut components, $x_{SRM}$ and $y_{SRM}$, providing the angles between the polished wafer surface and the Si crystal planes. The geometry of each of the miscut angles is provided in Figure 2.

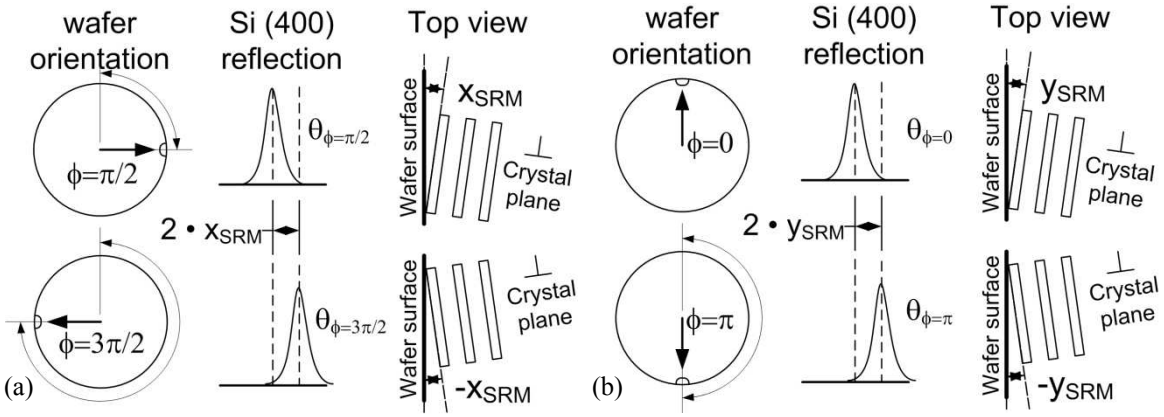


Figure 2. Schematic of wafer miscut from the Si crystal planes using measurements from two wafer orientations. A miscut is calculated for both the horizontal $x_{SRM}$ and the vertical $y_{SRM}$ wafer orientations. Figure 2(a) shows $x_{SRM}$ calculation parameters (see Equation 2). Figure 2(b) shows $y_{SRM}$ calculation parameters (see Equation 3).

$$x_{SRM} = \frac{\theta_{\pi/2} - \theta_{3\pi/2}}{2} \tag{2}$$

$$y_{SRM} = \frac{\theta_0 - \theta_\pi}{2} \tag{3}$$

By expressing the Cartesian miscut information, $x_{SRM}$ and $y_{SRM}$, in polar coordinates, we can provide the miscut information in azimuthal magnitude, $\xi_{SRM}$, and orientation, $\phi_{SRM}$ (see Figure 3). Equations 4 and 5 are used to calculate these quantities. Note that the miscut orientation is defined from the front of the sample, with the angle of the wafer notch setting $\phi_{SRM} = 0$ rad.

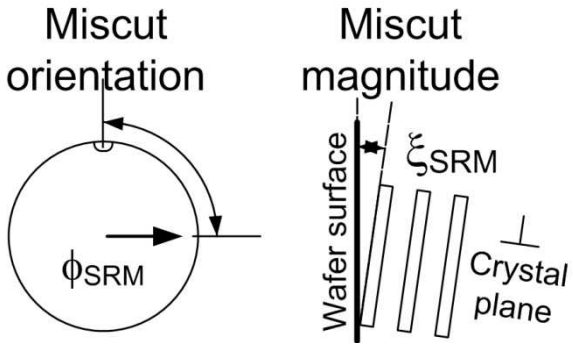


Figure 3. Schematic of wafer miscut polar coordinates showing miscut orientation, $\phi_{SRM}$, and miscut magnitude, $\xi_{SRM}$.

$$\xi_{SRM} = \arctan\sqrt{\tan^2 x_{SRM} + \tan^2 y_{SRM}} \tag{4}$$

$$\phi_{SRM} = \arctan\frac{\tan x_{SRM}}{\tan y_{SRM}} \tag{5}$$

**CERTIFICATION ANALYSIS**

*Calculating Si (220) transmission d-spacing:* With the effective wavelength known for each alignment of the system, calculating the *d*-spacing simply requires applying Bragg's law to pairs of dispersive and non-dispersive peak positions. A small correction for temperature is also required with which a small uncertainty, $u_c(\Delta Td) = 32$ am, is associated. These statistical calculations were performed in Python [26], R [27], and DATAPLOT [28] and then independently verified by the NIST Statistical Engineering Division (SED) using DATAPLOT.

Type A statistical uncertainty: The measured *d*-spacing for each SRM 2012 specimen varies because of statistical variation (from both instrument repeatability and sample *d*-spacing distribution) as well as systematic variation arising from the sample position on the CDPBD wafer holder. Because of the systematic nature of the variation with sample holder position, it was judged inappropriate to include this variation in the Type A statistical uncertainty ($k = 1$), $u_i(d_{SRM})$. One-way ANOVA was therefore used to separate the statistical variation from the systematic component by generating a correction to *d*-spacing based on sample position. The estimate of $d_{SRM}$ is then the mean of the set of estimates, and $u_i(d_{SRM}) = 0.24$ fm is determined as the residual standard deviation of the ANOVA model (that is, the variance not explained by the wafer holder position correction).

Type B systematic uncertainty related to misalignment: The only error relating to alignment that has a significant impact on the uncertainties for $d_{SRM}$ is the relative misalignment of the SRM feedstock and the reference crystal, $\Delta_{\delta_2}$. Such misalignment may cause a systematic error because the wafers and the reference crystals are mounted differently. Therefore, based on a study of misalignment effects, we assign a large maximum offset to *d*-spacing of $\Delta_{\delta_2} d \leq 0.62$ fm and so a standard uncertainty ($k = 1$) of $u_j(\Delta_{\delta_2} d) = 0.36$ fm.

*Best estimate and combined standard uncertainty*: The best estimate of the Si (220) substrate *d*-spacing of the SRM 2012 feedstock measured in transmission is $d_{SRM} = 0.192\,016\,1$ nm. The combined standard uncertainty ($k = 1$) of the SRM 2012 *d*-spacing is the combination of the statistical uncertainty computed above, the uncertainty of the misalignment difference between the SRM and the reference crystal, the temperature uncertainty in measuring the specimens, and the uncertainty in the reference crystal *d*-spacing from reference 5, $u_c(d_{WASO04}) = 12.1$ am.

$$u_c\left(d_{SRM}\right) = \sqrt{u_i\left(d_{SRM}\right)^2 + u_j\left(\Delta_{\delta_2} d\right)^2 + u_c\left(\delta_T d\right)^2 + u_c\left(d_{WASO04}\right)^2} \tag{6}$$

Thus the standard uncertainty ($k = 1$), $u_c(d_{SRM}) = 0.43$ fm. Expressed as a relative standard uncertainty ($k = 1$), $u_c(d_{SRM})/d_{SRM} = 2.2 \times 10^{-6}$. The expanded uncertainty ($k = 2$) is $U(d_{SRM}) = 0.87$ fm.

*Calculating surface-to-crystal-plane miscut best estimates and combined standard uncertainty:* The estimates used for the certified values are the means over all of the wafers, and the type A standard uncertainties are their estimated standard deviations over that set. Their values are given in Table 5.

*Calculating Bragg angle of Si (004) reflection best estimate and combined standard uncertainty:* Because of the effects of material index of refraction, wafer curvature, vertical divergence, long-range goniometer angle uncertainties, and other systematic corrections to reflection Bragg angle, certification of the *d*-spacing of the substrate in reflection condition is not possible at this time. Instead, to provide a traceable parameter for a reflection condition measurement of the SRM, we use the uncorrected Bragg angle of the Si (004) reflection diffraction peak from the surface of the wafer. This quantity can be calculated from the Bragg angle of the Si (004) reflection, $\theta_{B,SRM\,(004)}$, corrected for the miscut of the surface relative to the crystal planes (see Equation 7).

$$\theta_{surface,SRM(004)} = \theta_{B,SRM(004)} - x_{SRM} \tag{7}$$

Since only one Si (004) reflection case peak could be measured, to determine the uncorrected Bragg angle of the reflection requires knowledge of the angle of the diffracting planes of the crystal, $\Delta\theta_0$ (see Equation 8).

$$\theta_{B,SRM(004)} = \theta_{meas(004)} - \Delta\theta_0 \tag{8}$$

This is known in this case from the positions of the dispersive and non-dispersive transmission peaks (used in the *d*-spacing calculation of Equation 1).

$$\Delta\theta_0 = \frac{\theta_{meas(220)+} + \theta_{meas(220)-}}{2} - \frac{\pi}{2} \tag{9}$$

The Bragg angle of the Si (004) reflection was estimated for each sample position for each wafer; the mean and estimated standard deviation of this set are given in Table 6. Since temperature correction for *d*-spacing variation

cannot be applied directly to angle, an additional uncertainty ($k = 1$), $u_i(\Delta_T\theta_{B,SRM\,(004)}) = 0.50$ μrad, due to temperature variation over the course of the measurements must be incorporated. An uncertainty must be added due to long-range error of the goniometer, $u_j(\omega_{SRM}) = 3.9$ μrad at this angle. Finally, a correction for the uncertainty in NIST monochromator wavelength, $\lambda_{SRM}$ (see Table 7), and its corresponding contribution to the uncertainty of the Bragg angle ($k = 1$), $u_i(\lambda_{mono}\theta_{B,SRM\,(004)}) = 7.3$ rad, must be included. The resulting combined standard uncertainty ($k = 1$),

$$u_c(\theta_{B,SRM(004)}) = \sqrt{[u_i(\theta_{B,SRM(004)})^2 + u_i(\Delta_T\theta_{B,SRM(004)})^2 + u_j(\omega_{SRM})^2 + u_i(\lambda_{mono}\theta_{B,SRM(004)})^2]} = 11 \text{ μrad.}$$

The best estimate and uncertainties of the certified angle of the (004) reflection from the surface are given in Table 6.

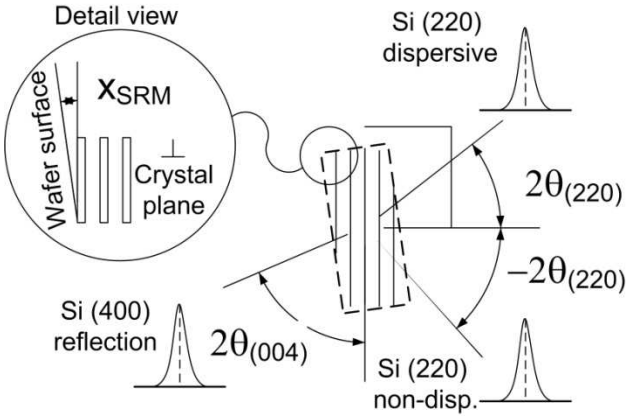


Figure 4. Top-view schematic of Si (004) reflection Bragg angle showing determination of crystal plane using Si (220) dispersive and non-dispersive peak positions and showing the miscut angle in the specimen x direction relating wafer surface with crystal plane, $x_{SRM}$.

**SI TRACEABILITY**

Uncertainty analyses performed for this SRM follow the ISO Guide to the Expression of Uncertainty in Measurement [2]. Figure 5 shows the SI traceability pathway for Si (220) *d*-spacing determination using SI-defined units of time, t, and distance, m, as input parameters [1,3,4]. This diagram illustrates the flow of SI units, the essential prior SI-traceable measurements, and the measured feedstock and material properties in an unbroken chain, as required for computing the total uncertainty budget in a given measurement. Three different feedstock Si boules and corresponding Si (220) *d*-spacings were used in the traceability chain for this SRM; (1) a purpose-commissioned boule of Si known as the WASO 4.2 feedstock provided the direct link to the SI through optical frequency via its use as the X-ray interferometer in the X-ray / optical interferometer at Physikalisch-Technische Bundesanstalt (PTB, Braunschweig, Germany) [5]; (2) a purpose-commissioned boule of Si used in the Avogadro Project, known as WASO 04 feedstock, provided reference artifacts for internal calibration of the NIST CDPBD instrument through direct comparison with WASO 4.2 on the NIST lattice comparator [29]; (3) a set of epitaxially-coated wafers sectioned from a single commercial CZ boule of Si, known as SRM 2012 feedstock, are the certified artifacts measured on the CDPBD by comparison with WASO 04.

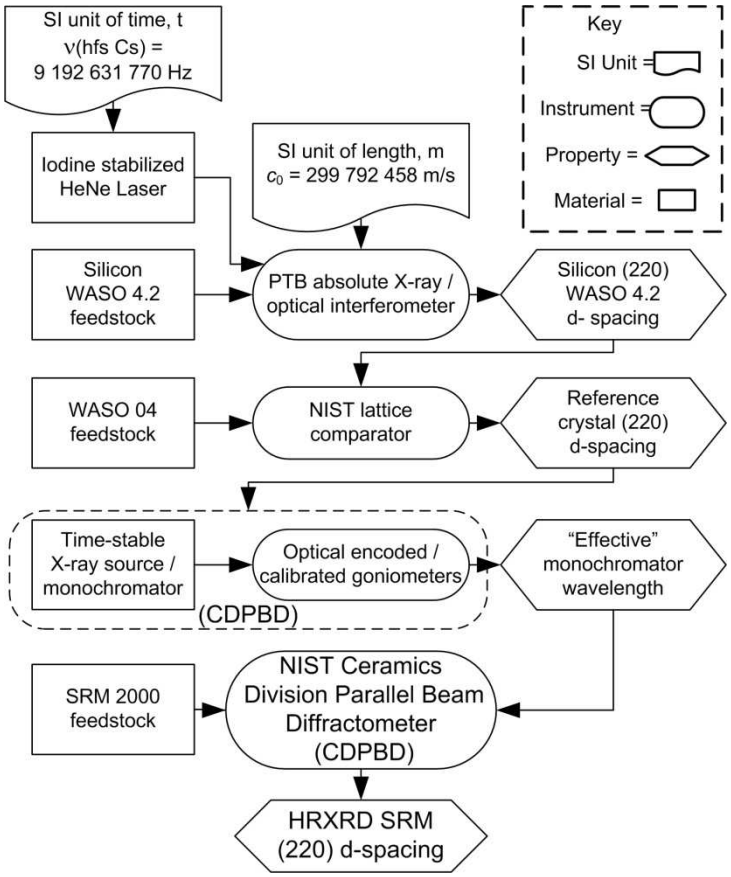


Figure 5: SI traceability pathway for Si (220) *d*-spacing in transmission.

## INSTRUCTIONS FOR HANDLING, STORAGE, AND USE

### Handling and Storage

The epitaxial layer can be damaged or the wafer strained mechanically; therefore contact with the front surface of the SRM wafer should be avoided. To remove surface contamination, use filtered nitrogen gas, or instrument-vendor wafer cleaning protocol.

*Peak profiles:* The measured diffraction peaks were significantly asymmetric. Supporting measurements suggest that this asymmetry may not be entirely due to instrument effects, but may be in part due to properties of the SRM 2012 feedstock. Therefore, a split-Pearson VII profile was used for fitting and estimating peak positions and is recommended for determining peak positions for calibration. Use of another profile function may result in systematic bias due to differing effects of asymmetry on profile position determination.

### Use

*Suggested use of d-spacing measured in Si (220) transmission:* Calibration by direct use of the certified *d*-spacing, $d_{SRM}$ requires an instrument that can measure in transmission geometry. If this is possible, one can calibrate either the instrument monochromator's wavelength, $\lambda_{inst}$, or angle measurements near the Si (220) reflection (in transmission geometry), $\Delta\theta_{inst}$. The following procedure provides an approach for this calibration (see Table 3 for scan ranges). Individual instrument manufacturers may have alternative suggested procedures.

1. Clean wafer holder and SRM with filtered nitrogen prior to mounting.
2. Mount SRM in holder with wafer notch upright and scribe marks facing away from source.
3. Locate non-dispersive Si (220) peak center, ω, using a setup scan.
4. Perform non-dispersive Si (220) normal range scan to measure peaks' full width at half maximum (FWHM).
5. Re-align wafer azimuth and repeat (4) until minimum FWHM is achieved.
6. Locate dispersive Si (220) peak center, ω, using a setup scan.
7. Perform dispersive Si (220) normal range scan to measure FWHM.
8. Locate Si (004) reflection peak center, ω, using a setup scan.
9. Perform a series of Si (004) reflection normal range scans at various wafer tilts, $\delta_2$ – defined as χ tilt on most instruments.

10. Set $\delta_2$ for wafer based on Si (004) reflection FWHM minimum.
11. Measure non-dispersive Si (220) HRXRD data.
12. Measure dispersive Si (220) HRXRD data.
13. Repeat steps 11 and 12.
14. Use difference of step 13 to determine $\theta_{\text{inst}(220)}$.
15. Use $\theta_{\text{inst}(220)}$ and $d_{\text{SRM}}$ to calibrate either $\lambda_{\text{inst}}$ or $\Delta\theta_{\text{inst}}$.

*Suggested use of surface-to-crystal-plane miscut:* The miscut certification will allow calibration and repeatability studies for rotating sample holders in commercial instruments in the field. By repeating miscut measurements on the SRM, one can test the repeatability and stability of a sample holder during rotation and remounting. The following procedure provides an approach for this sample holder calibration. Individual instrument manufacturers may have alternative suggested procedures.

1. Clean wafer holder and SRM with filtered nitrogen prior to mounting.
2. Mount SRM in holder with wafer notch upright and scribe marks facing away from source.
3. Measure Si (004) reflection HRXRD data at $\phi = 0$ rad.
4. Rotate sample to $\phi = \pi/2$ rad and measure Si (004) HRXRD data.
5. Rotate sample to $\phi = \pi$ rad and measure Si (004) HRXRD data.
6. Rotate sample to $\phi = 3\pi/2$ rad and measure Si (004) HRXRD data.
7. Calculate $x_{\text{inst}}$ using equation 2 and data from steps 4 and 6.
8. Calculate $y_{\text{inst}}$ using equation 3 and data from steps 3 and 5.
9. Calculate $\xi_{\text{inst}}$ and $\phi_{\text{inst}}$ using equations 4 and 5.
10. Compare values, $\xi_{\text{inst}}$ and $\phi_{\text{inst}}$, with certified values $\xi_{\text{SRM}}$ and $\phi_{\text{SRM}}$.
11. Use comparison data to align wafer holder.
12. Repeat steps 1 through 11 several times to reduce statistical uncertainty terms.

*Suggested use of Bragg angle of Si (004) reflection:* If transmission measurements are not possible, one can use the uncorrected Bragg angle of the Si (004) reflection, $\theta_{\text{B,inst}(004)}$, for calibration of either the instrument monochromator's wavelength, $\lambda_{\text{inst}}$ or angle measurements near the Si (004) reflection (in reflection geometry), $\Delta\theta_{\text{inst}}$. The following relational formula uses Bragg's law to relate the SRM and instrument parameters and may be used to solve for either quantity of interest using equation 7:

$$\lambda_{\text{inst}} \Big/ \sin(\theta_{\text{B,inst}(004)}) = \lambda_{\text{SRM}} \Big/ \sin(\theta_{\text{B,SRM}(004)}) \tag{10}$$

The following procedure provides an approach for this type of calibration. Additional uncertainties may result from differences in beam conditioning optics. Individual instrument manufacturers may have alternative suggested procedures.

1. Perform surface-to-crystal-plane misalignment calibration procedure.
2. Remount SRM in holder with serial number upright and facing sample holder.
3. Perform specular reflection alignment to determine specimen surface orientation with respect to the instrument plane.
4. Reset instrument ω zero to the wafer surface.
5. Measure Si (004) reflection HRXRD data at ϕ = 0 rad.
6. Use measured $\theta_{\text{surface,inst}(004)}$ and $\theta_{\text{surface,SRM}(004)}$ to calibrate either $\lambda_{\text{inst}}$ or $\Delta\theta_{\text{inst}}$.
7. Repeat steps 2 through 5 several times to reduce the uncertainty in statistical mounting errors.

The procedures for aligning the specular reflection will introduce significant uncertainties that must be included in any uncertainty budget for use of the certified values.

Table 4. Uncertainty Budget for SRM 2012 Si (220) *d*-Spacing

| Quantity | Standard Uncertainty ($k = 1$) | | Uncertainty Type |
|---|---|---|---|
| $d_{\text{SRM}}$ | 0.43 | fm | Combined, $u_c(i)$ |
| $d_{\text{SRM}}$ | 0.24 | fm | A, $u_i(i)$ |
| $\Delta_{\delta_2} d$ | 0.36 | fm | B, $u_j(i)$ |
| $\Delta_T d$ | 32 | am | Combined, $u_c(i)$ |
| $d_{\text{WASO04}}$ | 12 | am | Combined, $u_c(i)$ |

Table 5. Uncertainty Budget for SRM 2012 Si (220) Miscut

| Quantity | Standard Uncertainty ($k = 1$) | | Uncertainty Type |
|---|---|---|---|
| $\xi_{SRM}$ | 0.014 | mrad | Combined, $u_c(i)$ |
| $\phi_{SRM}$ | 7.9 | mrad | Combined, $u_c(i)$ |
| $x_{SRM}$ | 36 | µrad | Combined, $u_c(i)$ |
| $y_{SRM}$ | 9.5 | µrad | Combined, $u_c(i)$ |
| $\xi_{SRM}$ | 0.014 | mrad | A, $u_i(i)$ |
| $\phi_{SRM}$ | 7.9 | mrad | A, $u_i(i)$ |
| $x_{SRM}$ | 36 | µrad | A, $u_i(i)$ |
| $y_{SRM}$ | 9.5 | µrad | A, $u_i(i)$ |

Table 6. Uncertainty Budget for SRM 2012 Si (004) Surface Bragg Angle

| Quantity | Standard Uncertainty ($k = 1$) | | Uncertainty Type |
|---|---|---|---|
| $\theta_{surface,SRM(004)}$ | 38 | µrad | Combined, $u_c(i)$ |
| $x_{SRM}$ | 36 | µrad | A, $u_i(i)$ |
| $\theta_{B,SRM(004)}$ | 11 | µrad | Combined, $u_c(i)$ |
| $\theta_{surface,SRM(004)}$ | 7.3 | µrad | A, $u_i(i)$ |
| $\Delta_T\theta_{B,SRM(004)}$ | 0.5 | µrad | A, $u_i(i)$ |
| $\omega_{SRM}$ | 3.9 | µrad | B, $u_j(i)$ |
| $\lambda_{SRM}\theta_{B,SRM(004)}$ | 7.3 | µrad | B, $u_j(i)$ |

Table 7. Definitions used in SRM 2012 Uncertainty Analysis

| Quantity | Value | | Description |
|---|---|---|---|
| $u_i(d_{SRM})$ | 0.24 | fm | standard uncertainty ($k = 1$) (type A) of Si (220) transmission case *d*-spacing |
| $u_j(\Delta_{\delta_2}d)$ | 0.36 | fm | standard uncertainty (type B) due to misalignment between reference crystal and SRM feedstock |
| $u_c(\Delta_T d)$ | 0.032 | fm | combined standard uncertainty of *d*-spacing due to temperature effects |
| $u_c(d_{WASO04})$ | 12 | am | combined standard uncertainty of WASO 04 *d*-spacing determination |
| $u_i(\xi_{SRM})$ | 0.014 | mrad | standard uncertainty (type A) of magnitude of wafer miscut |
| $u_i(\phi_{SRM})$ | 7.9 | mrad | standard uncertainty (type A) of direction of wafer miscut |
| $u_i(x_{SRM})$ | 36 | µrad | standard uncertainty (type A) of tilt of wafer miscut in *x*-plane |
| $u_i(y_{SRM})$ | 9.5 | µrad | standard uncertainty (type A) of tilt of wafer miscut in *y*-plane |
| $u_i(x_{SRM})$ | see above | | see above |
| $u_c(\theta_{B,SRM(004)})$ | 8.0 | µrad | combined standard uncertainty of Bragg angle from crystal planes for Si (004) reflection peak |
| $u_i(\theta_{B,SRM(004)})$ | 7.3 | µrad | standard uncertainty (type A) of Bragg angle from crystal planes for Si (004) reflection peak |
| $u_i(\Delta_T\theta_{B,SRM(004)})$ | 0.5 | µrad | standard uncertainty (type A) due to temperature deviation over measurements |
| $\omega_{SRM}$ | 3.9 | µrad | standard uncertainty (type B) of long range error in ω axis at Si (004) |
| $\lambda_{SRM}$ | 154 055.9 | fm | reference monochromator wavelength for Si (004) measurements |
| $u_i(\lambda_{SRM}\theta_{B,SRM(004)})$ | 7.3 | µrad | standard uncertainty (type A) due to monochromator wavelength deviation over Si (004) measurements |

## REFERENCES


[1] *The International System of Units (SI)*; 8th ed.; Bureau International des Poids et Mesures, Paris (2006).

[2] JCGM 100:2008; *Evaluation of Measurement Data — Guide to the Expression of Uncertainty in Measurement* (ISO GUM 1995 with Minor Corrections); Joint Committee for Guides in Metrology (JCGM) (2008); available at *http://www.bipm.org/utils/common/documents/jcgm/JCGM_100_2008_E.pdf* (accessed Jan 2012); see also Taylor, B.N.; Kuyatt, C.E.; *Guidelines for Evaluating and Expressing the Uncertainty of NIST Measurement Results*; NIST Technical Note 1297; U.S. Government Printing Office: Washington, DC (1994); available at *http://www.nist.gov/pml/pubs/index.cfm* (accessed Jan 2012).

[3] Thompson, A.; Taylor, B.N.; *Guide for the Use of the International System of Units (SI)*; NIST Special Publication 811; U.S. Government Printing Office: Washington, DC (2008); available at *http://www.nist.gov/pml/pubs/index.cfm/* (accessed Jan 2012).
[4] ISO; *Quantities and Units*; 3rd ed.; ISO: Geneva, Switzerland (1993).
[5] Becker, P.; Bettin, H.; Danzebrink, H.U.; Glaser, M.; Kuetgens, U.; Nicolaus, A.; Schiel, D.; De Bievre, P.; Valkiers, S.; Taylor, P.; *Determination of the Avogadro constant via the silicon route*; Metrologia, Vol. 40(5), pp. 271–287 (2003).
[6] Hanke, M.; Kessler, E.G.; *Precise Lattice Parameter Comparison of Highly Perfect Silicon Crystals*; J. Phys. D: Appl. Phys., Vol. 38(10A), pp. A117–A120 (2005).
[7] Deslattes, R.D.; Kessler, E.G.; Owens, S.; Black, D.; Henins, A.; *Just how perfect can a perfect crystal be?*; J. Phys. D: Appl. Phys., Vol. 32(10A), pp. A3–A7 (1999).
[8] Becker, P.; *The determination of the Avogadro constant - not simply a metrological problem*; IEEE Transactions on Instrumentation and Measurement, Vol. 48(2), pp. 225–229 (1999).
[9] Becker, P.; Kuetgens, U.; Stumpel, J.; *The Avogadro Problem: Summary of Tests on Crystal Imperfections*; IEEE Transactions on Instrumentation and Measurement, Vol. 50(2), pp. 612–615 (2001).
[10] Bearden, J.A.; Thomsen, J.S.; Henins, A.; Sauder, W.C.; Marzolf, J.G.; *Precision Redetermination of Standard Reference Wavelengths for X-ray Spectroscopy*; Physical Review a - General Physics, Vol. 135(4A), p. A899 (1964).
[11] Azároff, L.V.; *X-ray Spectroscopy*; McGraw-Hill Book Company, NY (1974).
[12] Schnopper, H.W.; *Spectral Measurements with Aligned and Misaligned 2-Crystal Spectrometers. I. Theory of Geometrical Window*; J. Appl. Phys., Vol. 36(4), p. 1415 (1965).
[13] Schnopper, H.W.; *Spectral Measurements with Aligned and Misaligned 2-Crystal Spectrometers. II. Alignment*; J. Appl. Phys., Vol. 36(4), p. 1423 (1965).
[14] Bearden, J.A.; Thomsen, J.S.; *Double-crystal X-ray Spectrometer - Corrections, Errors, and Alignment Procedure*; J. of Appl. Cryst., Vol. 4, p. 130 (1971).
[15] Batterman, B.W.; Cole, H.; *Dynamical Diffraction of X-rays by Perfect Crystals*; Reviews of Modern Physics, Vol. 36(3), p. 681 (1964).
[16] Authier, A.; *Dynamical Theory of X-Ray Diffraction,* Oxford: Oxford University Press (2001).
[17] Bond, W.L.; *Precision Lattice Constant Determination*; Acta Crystallographica, Vol. 13(10), pp. 814–818 (1960).
[18] Walder, V.; Burke, J.; *Elimination of Specimen and Beam Tilt Errors in Bond Method of Precision Lattice Parameter Determinations*; J. Appl. Cryst., Vol. 4, p. 337 (1971).
[19] Halliwell, M.A.G.; *Measurement of Specimen Tilt and Beam Tilt in Bond Method*; J. Appl. Cryst., Vol. 3, p. 418 (1970).
[20] Burke, J.; Tomkeieff, M.V.; *Errors in Bond Method of Lattice Parameter Determinations-Further Considerations*; J. Appl. Cryst., Vol. 2, Part 6, p. 247 (1969).
[21] Hubbard, C.R.; Mauer, F.A.; *Precision and Accuracy of Bond Method as Applied to Small Spherical Crystals*; J. Appl Cryst.; Vol. 9, pp. 1–8 (1976).
[22] Prince, E.; *Mathematical, Physical and Chemical Tables*; Vol. C, International Tables for Crystallography, 3rd ed., London: Kluwer Academic (2004).
[23] Chantler, C.T.; *X-ray-Diffraction of Bent Crystals in Bragg Geometry .1. Perfect-Crystal Modeling*. J. Appl. Cryst., Vol. 25, Part 6, pp. 674–693 (1992).
[24] Chukhovskii, F.N.; Petrashen, P.V.; *General Dynamical Theory of X-ray Laue Diffraction from a Homogeneously Bent Crystal*; Acta Crystallographica, Vol. 33, Section A, pp. 311–319 (1977).
[25] Yan, H.; Kalenci, O.; Noyan, I.C.; *Diffraction Profiles of Elastically Bent Single Crystals with Constant Strain Gradients*; J. Appl. Cryst., Vol. 40, Part 2, pp. 322–331 (2007).
[26] Jones, E.; Oliphant, T.; Peterson, P.; and others. *SciPy: Open source scientific tools for Python* (2001).
[27] R Development Core Team; *A Language and Environment for Statistical Computing. R Foundation for Statistical Computing*; ISBN 3-900051-07-0, Vienna, Austria (2007).
[28] Heckert, N.A.; Filliben, J.J.; *NIST Handbook 148: DATAPLOT Reference Manual, Volume I: Commands*, National Institute of Standards and Technology Handbook Series, (2003); *http://www.itl.nist.gov/div898/software/dataplot.html/* (accessed Jan 2012).
[29] Kessler, E.G.; Owens, S.M.; Henins, A.; Deslattes, R.D.; *Silicon Lattice Comparisons Related to the Avogadro Project: Uniformity of New Material and Surface Preparation Effects*; IEEE Transactions on Instrumentation and Measurement, Vol. 48(2), pp. 221–224 (1999).

*Users of this SRM should ensure that the Certificate of Analysis in their possession is current. This can be accomplished by contacting the SRM Program: telephone (301) 975-2200; fax (301) 926-4751; e-mail srminfo@nist.gov; or via the Internet at http://www.nist.gov/srm.*